

Piezoelectric vibration damping using resonant shunt circuits: an exact solution

Soltani, P., Kerschen, G., Tondreau, G. & Deraemaeker, A.
Author post-print (accepted) deposited by Coventry University's Repository

Original citation & hyperlink:

Soltani, P, Kerschen, G, Tondreau, G & Deraemaeker, A 2014, 'Piezoelectric vibration damping using resonant shunt circuits: an exact solution' Smart Materials and Structures, vol. 23, no. 12, pp. 125014.

<https://dx.doi.org/10.1088/0964-1726/23/12/125014>

DOI 10.1088/0964-1726/23/12/125014

ISSN 0964-1726

ESSN 1361-665X

Publisher: IOP Publishing

Copyright © and Moral Rights are retained by the author(s) and/ or other copyright owners. A copy can be downloaded for personal non-commercial research or study, without prior permission or charge. This item cannot be reproduced or quoted extensively from without first obtaining permission in writing from the copyright holder(s). The content must not be changed in any way or sold commercially in any format or medium without the formal permission of the copyright holders.

This document is the author's post-print version, incorporating any revisions agreed during the peer-review process. Some differences between the published version and this version may remain and you are advised to consult the published version if you wish to cite from it.

Piezoelectric Vibration Damping using Resonant Shunt Circuits: An Exact Solution

Journal:	<i>Smart Materials and Structures</i>
Manuscript ID:	SMS-101020
Manuscript Type:	Paper
Date Submitted by the Author:	01-Jul-2014
Complete List of Authors:	Soltani, Payam; University of Liege, Kerschen, Gaetan; University of Liege, Tondreau, Gilles; Universite libre de Bruxelles, BATir Deraemaeker, Arnaud; Universite libre de Bruxelles, BATir
Article Keywords:	piezoelectric tuned vibration absorber, shunted piezoelectric transducer, optimum tuning rule, equal-peak method, exact closed-form solution
Abstract:	The objective of this paper is to propose an exact closed-form solution to the H_{∞} optimization of piezoelectric materials shunted with inductive-resistive passive electrical circuits. Realizing that Den Hartog's method which imposes fixed points of equal height in the receptance transfer function is approximate, the parameters of the piezoelectric vibration absorber are calculated through the direct minimization of the maxima of the receptance. The method is applied to a one-degree-of-freedom primary oscillator considering various values of the electromechanical coupling coefficients.

Piezoelectric Vibration Damping using Resonant Shunt Circuits: An Exact Solution

P. Soltani¹, G. Kerschen¹, G. Tondreau², A. Deraemaeker²

1. Space Structures and Systems Laboratory
Department of Aerospace and Mechanical Engineering
University of Liège, Liège, Belgium
E-mails: payam.soltani@ulg.ac.be, g.kerschen@ulg.ac.be

2. Building Architecture and Town Planning (BATir)
Université Libre de Bruxelles, Brussels, Belgium
E-mails: gilles.tondreau@ulb.ac.be, aderaema@ulb.ac.be

Abstract

The objective of this paper is to propose an exact closed-form solution to the H_∞ optimization of piezoelectric materials shunted with inductive-resistive passive electrical circuits. Realizing that Den Hartog's method which imposes fixed points of equal height in the receptance transfer function is approximate, the parameters of the piezoelectric tuned vibration absorber are calculated through the direct minimization of the maxima of the receptance. The method is applied to a one-degree-of-freedom primary oscillator considering various values of the electromechanical coupling coefficients.

Keywords: piezoelectric tuned vibration absorber, shunted piezoelectric transducer, optimum tuning rule, equal-peak method, exact closed-form solution.

Corresponding author:

Payam Soltani
Space Structures and Systems Laboratory
Department of Aerospace and Mechanical Engineering
University of Liège
1 Chemin des Chevreuils (B52/3), B-4000 Liège, Belgium.
E-mail: payam.soltani@ulg.ac.be.

1 Introduction

The mechanical tuned vibration absorber (MTVA) is probably the most popular passive anti-vibration device [1]. Successful applications of the MTVA can be found in civil engineering structures (e.g., the Burj Al Arab Hotel in Dubai, the Taipei World Financial Center in Taiwan and the Millenium Bridge in London) and in other engineering applications (e.g., cars and high-voltage lines). Different studies contributed to the development of analytic tuning procedures for the MTVA starting from the work of Den Hartog [2] and Brock [3] to the more recent contributions of Asami and Nishihara [4, 5].

An interesting alternative to the MTVA is the piezoelectric tuned vibration absorber (PTVA) implemented with a piezoelectric transducer (PZT) bonded to the structure and shunted with an electrical impedance. As the structure deforms, the PZT converts a portion of the mechanical energy into electrical energy which is in turn dissipated by the electrical circuit. Resonant circuit shunting is most often considered where the inherent capacitance of the PZT is shunted with a resistor and an inductor [6]. Linear [7, 8] and nonlinear [9, 10, 11] shunting strategies have been proposed in the literature. Even if they have their own limitations, PTVAs possess several advantages with respect to MTVAs, such as the absence of moving parts and the possibility to be fine-tuned online to compensate for any modeling errors. PTVAs are now enjoying applications in real-life structures such as bladed disk assemblies [12, 13].

Resonant circuit shunting enhances piezoelectric vibration damping through appropriate values of the frequency tuning and damping parameters. In [7], two different methods were proposed relying on the receptance transfer function and on pole placement, respectively. The former rule extends Den Hartog's fixed-point method [2] to PTVAs and is widely used in the literature [14]. Minimization of the frequency response amplitude is achieved by selecting the frequency tuning parameter that gives two fixed points in the receptance of the primary structure of equal heights. The later rule maximizes the attainable modal damping by finding the value of the frequency tuning parameter for which the distinct poles coalesce in double complex conjugate pairs. Hogsberg and Krenk recently proposed a tuning rule that is a balanced compromise between these two design criteria [15]. Through the development of an equivalent mechanical model of a piezoelectric element, Yamada et al. [16] introduced a new approximate analytic expression for the damping parameter that improves the PTVA performance compared to the formulae proposed in [7].

Because all the aforementioned tuning rules are approximate, the contribution of the present paper is to derive an exact closed-form solution for the design of piezoelectric vibration absorbers based on resonance circuit shunting. The paper is organized as follows. Section 2 briefly reviews Den Hartog's fixed-point method for MTVAs together with the exact solution proposed by Asami and Nishihara [4]. In Section 3, the formulation for shunted PZTs is introduced, and the tuning rules proposed by Hagood and von Flotow [7] and Yamada and co-workers [16] are discussed. An exact tuning rule for PTVAs is derived in Section 4 and compared to the other tuning rules using a one-degree-of-freedom mechanical oscillator. Simplified, though very accurate, formulae for the optimum frequency ratio and damping parameters are provided in Section 5. Finally, the conclusions of the present study are drawn in Section 6.

2 The mechanical tuned vibration absorber

The steady-state response of an undamped mass-spring system subjected to a harmonic excitation at a constant frequency can be suppressed using an undamped tuned vibration absorber (TVA), as proposed by Frahm in 1909 [17]. However, the TVA performance deteriorates significantly when the excitation frequency varies. To improve the performance robustness, damping was introduced in the absorber by Ormondroyd and Den Hartog [18]. The equations of motion of the coupled system are

$$\begin{aligned} m_1\ddot{x} + k_1x + c_2(\dot{x} - \dot{y}) + k_2(x - y) &= f \sin \omega t \\ m_2\ddot{y} + c_2(\dot{y} - \dot{x}) + k_2(y - x) &= 0, \end{aligned} \quad (1)$$

where $x(t)$ and $y(t)$ are the displacements of the harmonically-forced undamped primary system and of the MTVA, respectively. k_1 and k_2 are the stiffness of the primary structure and of the MTVA, in that order. c_2 represents the damping of the MTVA.

Den Hartog demonstrated that the receptance $g_m(\omega)$ of the primary mass passes through two fixed points independent of absorber damping, as illustrated in Figure 1. He proposed a tuning rule that provides two fixed points of equal height in the receptance curve [2]. Brock then computed the optimum damping by taking the mean of the damping values that realize a maximum of the receptance at the two fixed points [3]. The corresponding analytic formulae for the frequency tuning δ_m and damping ξ_2 ratios are:

$$\begin{aligned} \delta_m &= \frac{\omega_2}{\omega_1} = \frac{1}{1 + \beta} \\ \xi_2 &= \frac{c_2}{2\sqrt{k_2m_2}} = \sqrt{\frac{3\beta}{8(1 + \beta)}}, \end{aligned} \quad (2)$$

where ω_1 and ω_2 are the natural frequencies of the primary system and of the absorber, respectively, $\beta = m_2/m_1$ is the mass ratio and ξ_2 is the damping ratio. Table 1 shows that the two fixed points have the same amplitudes, unlike the two maxima of the receptance curve. Even though they have most likely sufficient accuracy considering the uncertainty inherent to practical applications, formulas (2) are therefore only approximate.

Interestingly, it is only recently that an exact closed-form solution to this classical problem could be found [4]. Instead of imposing two fixed points of equal amplitude, the direct minimization of the H_∞ norm of the frequency response of the controlled structure is achieved:

$$\min \|g_m(\omega)\|_\infty \rightarrow |g_m(\omega_A)| = |g_m(\omega_B)| \quad (3)$$

where ω_A and ω_B represent the resonance frequencies. Eventually, exact analytic formulas can be obtained for the frequency tuning and damping ratios:

$$\begin{aligned} \delta_m &= \frac{2}{1 + \beta} \sqrt{\frac{2 [16 + 23\beta + 9\beta^2 + 2(2 + \beta)\sqrt{4 + 3\beta}]}{3(64 + 80\beta + 27\beta^2)}} \\ \xi_2 &= \frac{1}{4} \sqrt{\frac{8 + 9\beta - 4\sqrt{4 + 3\beta}}{1 + \beta}} \end{aligned} \quad (4)$$

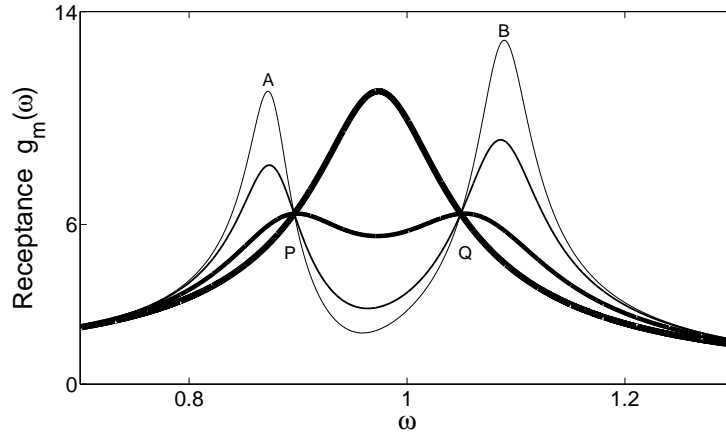


Figure 1: Illustration of Den Hartog’s fixed-point method for $\beta = 0.05$, $\delta_m = 0.952$ and for various absorber damping values ($\xi_2 = 0.0447$, $\xi_2 = 0.067$, $\xi_{2,opt} = 0.134$ and $\xi_2 = 0.268$; line thicknesses are proportion to ξ_2).

Table 1: Amplitude of the fixed-points and maxima of the receptance transfer function for Den Hartog’s tuning rule ($m_1 = 1$ kg and $k_1 = 1$ N/m).

Mass ratio	Fixed point P	Fixed point Q	Maximum A	Maximum B
0.05	6.4031	6.4031	6.4075	6.4084
0.1	4.5826	4.5826	4.5884	4.5902
0.5	2.2361	2.2361	2.2453	2.2530
1.0	1.7321	1.7321	1.7417	1.7544

Table 2: Amplitude of the fixed-points and maxima of the receptance transfer function for Asami and Nishihara’s tuning rule ($m_1 = 1$ kg and $k_1 = 1$ N/m).

Mass ratio	Fixed point P	Fixed point Q	Maximum A	Maximum B
0.05	6.4027	6.4035	6.4079	6.4079
0.1	4.5819	4.5833	4.5892	4.5892
0.5	2.2334	2.2387	2.2480	2.2480
1.0	1.7281	1.7360	1.7456	1.7456

Table 2 confirms that this tuning rule yields resonance peaks of equal amplitude. It also shows that, for this optimum design, the fixed points of the receptance curve do not have the same amplitude.

We note that all the developments in this section assume an undamped primary system. To date, there is no exact solution for damped primary systems, but accurate approximate analytic formulas have been derived [5].

3 The piezoelectric vibration absorber: existing tuning rules

3.1 Governing equations of structures with shunted piezoelectric materials

Because we aim at mitigating one specific structural resonance, a one-degree-of-freedom modal model of the host structure, assumed to be undamped, is considered to which a shunted piezoelectric transducer is attached. The PZT shunt is a series RL circuit. This system is schematized in Figure 2.

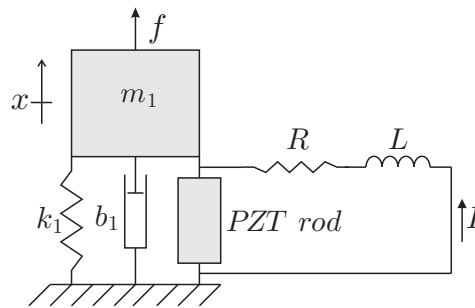


Figure 2: Piezoelectric vibration absorber with a series RL shunt.

Assuming linear characteristics under constant temperature, the general form of the piezoelectric constitutive equations are standardized by IEEE [19]:

$$\begin{aligned} \mathbf{S} &= [d] \mathbf{E} + [s^E] \mathbf{T}, \\ \mathbf{D} &= [\epsilon^T] \mathbf{E} + [d]^* \mathbf{T}. \end{aligned} \quad (5)$$

where \mathbf{T} and \mathbf{S} are the material stress and strain vectors, respectively; $[s^E]$ is the compliance matrix of the piezoceramic under constant electric field; $[\epsilon^T]$ represents the permittivity under constant stress; $[d]$ is the matrix of piezoelectric constants, and $*$ denotes matrix transpose. The components of the aforementioned vectors and matrices are defined

as [7]:

$$\mathbf{S} = \begin{Bmatrix} S_{11} \\ S_{22} \\ S_{33} \\ 2S_{23} \\ 2S_{31} \\ 2S_{12} \end{Bmatrix}, \mathbf{T} = \begin{Bmatrix} T_{11} \\ T_{22} \\ T_{33} \\ T_{23} \\ T_{31} \\ T_{12} \end{Bmatrix}, \mathbf{E} = \begin{Bmatrix} E_1 \\ E_2 \\ E_3 \end{Bmatrix}, \mathbf{D} = \begin{Bmatrix} D_1 \\ D_2 \\ D_3 \end{Bmatrix}, [d] = \begin{bmatrix} 0 & 0 & d_{31} \\ 0 & 0 & d_{32} \\ 0 & 0 & d_{33} \\ 0 & d_{24} & 0 \\ d_{15} & 0 & 0 \\ 0 & 0 & 0 \end{bmatrix},$$

$$[\epsilon^T] = \begin{bmatrix} \epsilon_1^T & 0 & 0 \\ 0 & \epsilon_2^T & 0 \\ 0 & 0 & \epsilon_3^T \end{bmatrix}, [s^E] = \begin{bmatrix} s_{11}^E & s_{12}^E & s_{13}^E & 0 & 0 & 0 \\ s_{21}^E & s_{22}^E & s_{23}^E & 0 & 0 & 0 \\ s_{31}^E & s_{32}^E & s_{33}^E & 0 & 0 & 0 \\ 0 & 0 & 0 & s_{44}^E & 0 & 0 \\ 0 & 0 & 0 & 0 & s_{55}^E & 0 \\ 0 & 0 & 0 & 0 & 0 & s_{66}^E \end{bmatrix}. \quad (6)$$

The current problem considers the PZT rod as a one-dimensional element in which both the expansion and polarization direction coincidence with the central axis of the rod (conventionally called the “3”-direction). Hence, the PZT rod operates in its thickness transduction mode or d_{33} -mode. The constitutive equations of the PZT rod then become:

$$\begin{Bmatrix} D_3 \\ S_{33} \end{Bmatrix} = \begin{bmatrix} \epsilon_3^T & d_{33} \\ d_{33} & s_{33}^E \end{bmatrix} \begin{Bmatrix} E_3 \\ T_3 \end{Bmatrix}. \quad (7)$$

By integrating Equations (7) over the volume of the PZT rod, the charge q and the displacement x are written as functions of the force f_{PZT} and the voltage between the electrodes v_{PZT} :

$$\begin{Bmatrix} q \\ x \end{Bmatrix} = \begin{bmatrix} c_{PZT} & d_{33} \\ d_{33} & \frac{1}{k_{PZT}} \end{bmatrix} \begin{Bmatrix} v_{PZT} \\ f_{PZT} \end{Bmatrix}. \quad (8)$$

The coefficient c_{PZT} is the capacitance between the electrodes of the PZT rod with no external force, and k_{PZT} is the stiffness of the short-circuited PZT rod. They are defined as:

$$c_{PZT} = \epsilon_3^T \frac{s_0}{l_0}, \quad k_{PZT} = \frac{1}{s_{33}^E} \frac{s_0}{l_0}, \quad (9)$$

where s_0 and l_0 are the cross section area and length of the PZT rod, respectively. Equation (8) can be reformulated as:

$$\begin{Bmatrix} v_{PZT} \\ f_{PZT} \end{Bmatrix} = \begin{bmatrix} \frac{1}{\bar{c}_{PZT}} & -\theta \\ -\theta & \bar{k}_{PZT} \end{bmatrix} \begin{Bmatrix} q \\ x \end{Bmatrix}. \quad (10)$$

where

$$\bar{c}_{PZT} = c_{PZT}(1 - k_0^2), \quad \bar{k}_{PZT} = \frac{k_{PZT}}{1 - k_0^2}, \quad \theta = \frac{k_0}{1 - k_0^2} \sqrt{\frac{k_{PZT}}{c_{PZT}}}, \quad (11)$$

are the capacitance of the PZT rod under constant strain, the stiffness of the PZT rod with open electrodes, and the electromechanical coupling factor θ , respectively. These parameters are defined as functions of the electromechanical coupling coefficient in d_{33} -mode:

$$k_0 = d_{33} \sqrt{\frac{k_{PZT}}{c_{PZT}}} = d_{33} \frac{1}{\sqrt{s_{33}^E \epsilon_3^T}}. \quad (12)$$

Finally, placing a resistive-inductive (RL) shunt across the electrodes of the piezoelectric and applying Newton's and Kirchhoff's law yield the governing equations of the system:

$$\begin{aligned} m_1 \ddot{x} + (k_1 + \bar{k}_{PZT}) x - \theta q &= f \sin \omega t \\ L \ddot{q} + R \dot{q} + \bar{c}_{PZT}^{-1} q - \theta x &= 0, \end{aligned} \quad (13)$$

where the primary host structure is considered undamped (i.e. $b_1 = 0$). By defining the parameters similarly than Ref.[9]:

$$\begin{aligned} \omega_1 &= \sqrt{\frac{k_1 + \bar{k}_{PZT}}{m_1}}, & \omega_e &= \frac{1}{\sqrt{L \bar{c}_{PZT}}}, & \gamma &= \frac{\omega}{\omega_1}, & \delta &= \frac{\omega_e}{\omega_1}, \\ \tilde{x} &= \sqrt{m_1} x, & \tilde{q} &= \sqrt{L} q, & r &= R \bar{c}_{PZT} \omega_1, \\ \tau &= \omega_1 t, & f_0 &= \frac{f}{\omega_1 \sqrt{\bar{k}_{PZT} + k_1}}, & \alpha &= \theta \sqrt{\frac{\bar{c}_{PZT}}{\bar{k}_{PZT} + k_1}}, \end{aligned} \quad (14)$$

Equations (13) can be conveniently recast into

$$\begin{aligned} \tilde{x}'' + \tilde{x} - \delta \alpha \tilde{q} &= f_0 \sin \gamma \tau \\ \tilde{q}'' + r \delta^2 \tilde{q}' - \delta \alpha \tilde{x} + \delta^2 \tilde{q} &= 0, \end{aligned} \quad (15)$$

where prime denotes differentiation with respect to the dimensionless time τ . We note that the parameter

$$\alpha = \theta \sqrt{\frac{\bar{c}_{PZT}}{\bar{k}_{PZT} + k_1}} = \sqrt{\frac{k_0^2}{1 - k_0^2}} \sqrt{\frac{k_{PZT}}{\bar{k}_{PZT} + k_1}} = k_0 \sqrt{\frac{\bar{k}_{PZT}}{\bar{k}_{PZT} + k_1}} = \frac{k_0}{\sqrt{1 + \kappa}}, \quad (16)$$

depends only on the stiffness ratio $\kappa = k_1/\bar{k}_{PZT}$ and the electromechanical coupling coefficient k_0 . Since PZT rods typically have $k_0 \cong 0.7$ in d_{33} -mode, α takes values between 0 and 0.7. It is related to the generalized electromechanical coupling coefficient K_{ij} defined in [7] according to the relation

$$K_{ij} = \sqrt{\frac{k_0^2}{1 - k_0^2}} \sqrt{\frac{k_{PZT}}{\bar{k}_{PZT} + k_1}} \rightarrow K_{ij} = \alpha \sqrt{\frac{1 + \kappa}{1 - k_0^2 + \kappa}} \quad (17)$$

3.2 Tuning rules for resonant shunt circuits

Given a value of the parameter α , the tuning of a RL shunt requires to determine the frequency tuning δ and damping r parameters. As briefly discussed in the introductory section, different rules exist for finding appropriate values of these parameters. Two methods that apply Den Hartog's fixed-point method to PTVAs, namely those of Hagood and von Flotow [7] and Yamada et al. [16], are described in this section.

3.2.1 Hagood's tuning rule

In 1991, Hagood and von Flotow introduced the first tuning method for resonant shunt circuits based on the receptance transfer function of the primary mass:

$$g_e(\gamma) = \left| \frac{\tilde{x}}{f_0} \right| = \left| \frac{j\delta^2 r\gamma + \delta^2 - \gamma^2}{\gamma^4 - j\delta^2 r\gamma^3 - (\delta^2 + 1)\gamma^2 + j\delta^2 r\gamma + (1 - \alpha^2)\delta^2} \right|, \quad (18)$$

with $j = \sqrt{-1}$. Since then, this method has often been used in the literature (e.g., Inman and co-workers applied the method for tuning the linear part of the proposed nonlinear piezoelectric shunt [9]).

The first step consists in selecting the frequency tuning parameter δ that yields two fixed points of equal amplitude in the receptance $g_e(\gamma)$. Solving the equation:

$$g_e(\gamma)|_{r=0} = g_e(\gamma)|_{r=\infty}, \quad (19)$$

yields the dimensionless frequencies of the fixed points P and Q :

$$\gamma_{P,Q} = \frac{\sqrt{2}}{2} \frac{\sqrt{\delta^2 + 1 \pm \sqrt{\delta^4 + 2\delta^2\alpha^2 - 2\delta^2 + 1}}}{\delta}. \quad (20)$$

The optimum value $\delta_{opt} = 1$ is subsequently obtained by imposing

$$g_e(\gamma_{P,Q}) = g_e(\gamma_{P,Q})|_{r=\infty}. \quad (21)$$

Because the parameters (14) are somewhat different from those considered in [7], the value of δ_{opt} is also different. At the optimum, the frequency of the fixed points and the corresponding amplitudes of the transfer function are

$$\gamma_{P,Q} = \frac{\sqrt{2}}{2} \sqrt{2 \pm \sqrt{2}\alpha} \quad \text{and} \quad g_e(\gamma_P) = g_e(\gamma_Q) = \frac{\sqrt{2}}{\alpha} \quad (22)$$

Determining the optimal circuit damping is more challenging. To this end, Hagood and von Flotow proposed to set

$$g_e(\gamma_{P,Q}) = g_e(\delta_{opt}). \quad (23)$$

As we shall see, this expression is approximate. Combining Equations (18), (22b) and (23) yields

$$r_{opt_H} = \sqrt{2}\alpha \quad (24)$$

3.2.2 Yamada's tuning rule

Through the development of an equivalent mechanical model of a piezoelectric element, Yamada et al. [16] improved the analytic approximations proposed in [7]. Specifically, they still consider the value $\delta_{opt} = 1$ for the frequency tuning, but the damping ratio of the PTVA is derived such that the derivative of the receptance $g_e(\gamma)$ should be zero at the fixed points:

$$\frac{dg_e(\gamma)}{d\gamma} \Big|_{\gamma_P, \gamma_Q} = 0. \quad (25)$$

By substituting Equation (22) into Equation (25), two different optimum circuit damping values are calculated for points P and Q :

$$r_{P,Q} = \frac{\sqrt{3}}{\sqrt[4]{2}} \frac{\alpha}{\sqrt{\sqrt{2} \pm \alpha}}. \quad (26)$$

meaning that the two maxima of $g_e(\gamma)$ cannot simultaneously coincide with the fixed points. They proposed to define the optimum value through the root mean square:

$$r_{optY} = \sqrt{\frac{r_P^2 + r_Q^2}{2}} = \frac{\sqrt{3}\alpha}{\sqrt{2 - \alpha^2}}. \quad (27)$$

The performance of the two tuning rules are illustrated in Figure 3 for different dimensionless coupling parameters α . For $\alpha=0.1$, the rule proposed by Yamada et al. provides two peaks of almost identical amplitudes, whereas the rule of Hagood and von Flotow is less accurate. For larger values of α , none of these rules provides equal peaks in the receptance function.

4 The piezoelectric vibration absorber: exact tuning rule

4.1 Theory

As discussed in Section 2 for MTVAs and as also shown in the previous section, a fixed-point-based absorber design cannot yield resonance peaks of equal amplitude. Following the method proposed by Nishihara and Asami [4] for MTVAs, an exact solution for the H_∞ optimization of piezoelectric materials shunted with resistive-inductive passive electrical circuits is derived in this section. It is obtained by focusing only on the resonant points A and B , therefore ignoring the existence of the fixed points. So, for a given value of α ,

$$\min_{\delta,r} \|g_e(\gamma)\|_\infty \rightarrow \text{find } \delta, r \text{ such that } |g_e(\gamma_A)| = |g_e(\gamma_B)| \equiv h_0 \quad (28)$$

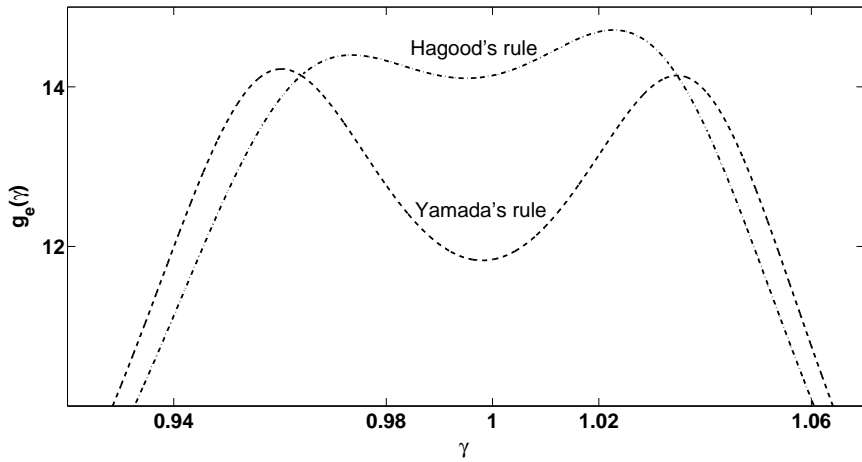
For simplicity, the square of the receptance function $g_e^2(\gamma) = n(\gamma)/d(\gamma)$ is considered where

$$n(\gamma) = 1 + \gamma^4 + (\delta^2 r^2 - 2) \gamma^2, \quad (29)$$

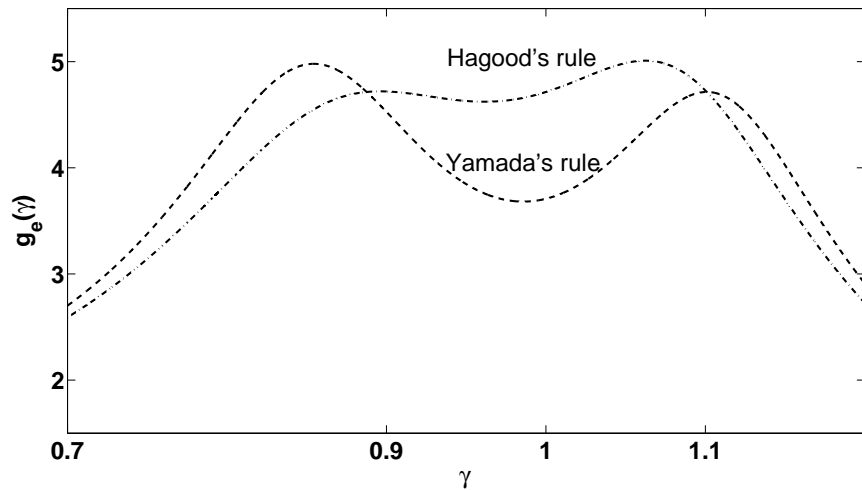
$$d(\gamma) = \delta^4 \gamma^8 + (\delta^6 r^2 - 2\delta^4 - 2\delta^2) \gamma^6 + (-2\delta^4 r^2 - 2\alpha^2 \delta^2 + \delta^4 + 4\delta^2 + 1) \gamma^4 + (2\alpha^2 \delta^2 + \delta^2 r^2 + 2\alpha^2 - 2\delta^2 - 2) \gamma^2 + \alpha^4 - 2\alpha^2 + 1. \quad (30)$$

Because only terms of even power appear in these expressions, we can pose $\gamma_1 = \gamma^2$ such that $g_e^2(\gamma_1) = N(\gamma_1)/D(\gamma_1)$ with

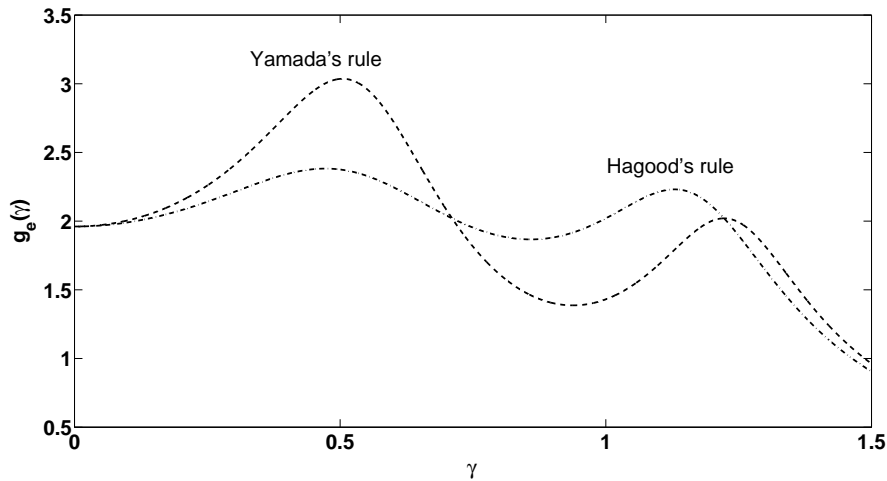
$$\begin{aligned} N(\gamma_1) &= 1 + \gamma_1^2 + (\delta^2 r^2 - 2) \gamma_1, \\ D(\gamma_1) &= \delta^4 \gamma_1^4 + (\delta^6 r^2 - 2\delta^4 - 2\delta^2) \gamma_1^3 + (-2\delta^4 r^2 - 2\alpha^2 \delta^2 + \delta^4 + 4\delta^2 + 1) \gamma_1^2 \\ &\quad + (2\alpha^2 \delta^2 + \delta^2 r^2 + 2\alpha^2 - 2\delta^2 - 2) \gamma_1 + \alpha^4 - 2\alpha^2 + 1. \end{aligned} \quad (31)$$



(a) $\alpha = 0.1$,
 $r_{opt_Y} = 0.1184$, $r_{opt_H} = 0.1414$, $\delta = 1$.



(b) $\alpha = 0.3$,
 $r_{opt_Y} = 0.3337$, $r_{opt_H} = 0.4243$, $\delta = 1$.



(c) $\alpha = 0.7$,
 $r_{opt_Y} = 0.7012$, $r_{opt_H} = 0.9899$, $\delta = 1$.

Figure 3: Performance of existing tuning rules for PTVAFs for different values of α .

If we define the fourth-order polynomial

$$F(\gamma_1) = D(\gamma_1) - \frac{N(\gamma_1)}{h_0^2}, \quad (32)$$

Equation (28) shows that two obvious roots of this polynomial are γ_{1A} and γ_{1B} . Because the receptance transfer function possesses horizontal tangents at the resonant points A and B , it also follows that

$$F'(\gamma_{1A}) = F'(\gamma_{1B}) = 0, \quad (33)$$

where prime represents the derivative with respect to γ_1 . According to Equation (33), the multiplicity of the roots γ_{1A} and γ_{1B} is two:

$$F(\gamma_1) = \gamma_1^4 + b_1\gamma_1^3 + b_2\gamma_1^2 + b_3\gamma_1 + b_4 = (\gamma_1 - \gamma_{1A})^2(\gamma_1 - \gamma_{1B})^2, \quad (34)$$

with the coefficients b_i defined as

$$\begin{aligned} b_1 &= -2(\gamma_{1A} + \gamma_{1B}), \\ b_2 &= (\gamma_{1A} + \gamma_{1B})^2 + 2\gamma_{1A}\gamma_{1B}, \\ b_3 &= -2\gamma_{1A}\gamma_{1B}(\gamma_{1A} + \gamma_{1B}), \\ b_4 &= \gamma_{1A}^2\gamma_{1B}^2. \end{aligned} \quad (35)$$

It follows that

$$\begin{aligned} f_1 &= b_1\sqrt{b_4} - b_3 = 0, \\ f_2 &= \frac{b_1^2}{4} + 2\sqrt{b_4} - b_2 = 0. \end{aligned} \quad (36)$$

Another expression of the coefficients b_i can be obtained through Equations (31) and (32):

$$\begin{aligned} b_1 &= -2 - 2\delta_1 + \frac{r_1}{\delta_1}, \\ b_2 &= \delta_1^2 h_1^2 + (4 - 2\alpha_1)\delta_1 - 2r_1 + 1, \\ b_3 &= \delta_1 [(-2h_1^2 + 2\alpha_1)\delta_1 + h_1^2 r_1 + 2\alpha_1 - 2], \\ b_4 &= \delta_1^2 (h_1^2 + \alpha_1^2 - 2\alpha_1). \end{aligned} \quad (37)$$

where $h_1^2 = 1 - 1/h_0^2$, $\delta_1 = 1/\delta^2$, $r_1 = r^2$ and $\alpha_1 = \alpha^2$. Equations (36) therefore becomes

$$f_1 = (-2\delta_1^2 + r_1 - 2\delta_1)\chi - \delta_1 [(-2h_1^2 + 2\alpha_1)\delta_1 + h_1^2 r_1 + 2\alpha_1] = 0, \quad (38)$$

$$f_2 = (1 - h_1^2)\delta_1^4 + 2(\chi + \alpha_2 - 1)\delta_1^3 + r_1\delta_1^2 - r_1\delta_1 + \frac{1}{4}r_1^2 = 0. \quad (39)$$

where $\chi \equiv \sqrt{h_1^2 + \alpha_1^2 - 2\alpha_1}$.

Equation (38) is solved for r_1 equal to the square of the optimum circuit damping:

$$r_1 = \frac{2\delta_1 [-\delta_1 h_1^2 + \delta_1 \chi + \delta_1 \alpha_1 + \chi + \alpha_1 - 1]}{-\delta_1 h_1^2 + \chi}. \quad (40)$$

The substitution of r_1 into Equation (39) provides a fourth-order polynomial in δ_1 , which is directly related to the frequency tuning ratio δ :

$$\tilde{a} \delta_1^4 + \tilde{b} \delta_1^3 + \tilde{c} \delta_1^2 + \tilde{d} \delta_1 + \tilde{e} = 0 \quad (41)$$

The coefficients of the polynomial depend only on α_1 , related to the coupling factor α , and h_1 , related to the amplitude h_0 of the receptance function:

$$\begin{aligned} \tilde{a} &= [h_1^4 (1 - h_1^2)], \\ \tilde{b} &= \left[4h_1^2 (1 - h_1^2) \left(\chi + \frac{1}{2} \alpha_1 \right) \right], \\ \tilde{c} &= \left[((-4\chi - 2) \alpha_1 - 5\chi^2 + 2) h_1^2 + 4 \left(\chi + \frac{1}{2} \alpha_1 \right)^2 - h_1^4 \right], \\ \tilde{d} &= [2\chi^3 + 2\chi^2 \alpha_1 + (2h_1^2 + 4\alpha_1 - 4) \chi + 2\alpha_1^2 - 2\alpha_1], \\ \tilde{e} &= [(\alpha_1 - 1)^2 - \chi^2]. \end{aligned} \quad (42)$$

The parameter α_1 is an input to the problem whereas h_1 should be minimized so as to minimize the resonance peak amplitude h_0 .

To ensure the existence of a multiple real root of Equation (41), the value of h_1 should be selected so that the discriminant of this polynomial Δ_4 is zero. For a n^{th} -order polynomial $f(x)$, a linear relation exists between the discriminant and the resultant $R(f, \frac{\partial f}{\partial x})$. This relation can be written for the quartic function f_2 as:

$$\Delta_4 = \frac{1}{\tilde{a}} R \left(f_2, \frac{\partial f_2}{\partial \delta_1} \right). \quad (43)$$

Hence, the resultant R can be set to zero instead of Δ_4 . Since the expression of R is very complex and cannot be solved by hand, the symbolic algebraic software Maple is used to simplify the resultant as:

$$\frac{1}{64} [54\alpha_1^3 - 54\alpha_1^2 + (144h_1^2 - 144)\alpha_1 - 128h_1^2 + 128] \sqrt{h_1^2 + \alpha_1^2 - 2\alpha_1} + \frac{27}{32} \alpha_1^4 - \frac{27}{16} \alpha_1^3 + \frac{1}{64} (171h_1^2 - 117) \alpha_1^2 + \frac{272}{64} (1 - h_1^2) \alpha_1 + h_1^4 - 1 = 0. \quad (44)$$

The common factor $1024\alpha_1^4 (h_1^2 - 1)^3 h_1^{10} [(h_1^2 + \chi) \alpha_1 - h_1^2 + \chi^2]^2$ was eliminated from the resultant during the simplifications. Four different roots are found for Equation (44):

$$h_1 = \pm \frac{1}{8} \sqrt{-9\alpha_1^2 - 16\alpha_1 + 64 \pm 2 \sqrt{54\alpha_1^4 - 144\alpha_1^3 + 64\alpha_1^2}} \quad (45)$$

Considering that h_1 should be positive and should be minimized, the following root is the solution:

$$h_{1opt} = \frac{1}{8} \sqrt{-9\alpha_1^2 - 16\alpha_1 + 64 - 2 \sqrt{54\alpha_1^4 - 144\alpha_1^3 + 64\alpha_1^2}} \quad (46)$$

This value of h_1 should be inserted into Equation (42) to obtain the coefficients in terms of α_1 , and Equation(41) can be solved analytically for δ_1 . Eventually:

$$\delta_{1opt} = \frac{4S\tilde{a} - \tilde{b}}{4\tilde{a}}. \quad (47)$$

where

$$S = \frac{1}{2} \sqrt{\frac{1}{3\tilde{a}} \left(Q + \frac{\Delta_0}{Q} \right) - \frac{2}{3}p}, \quad p = \frac{8\tilde{a}\tilde{c} - 3\tilde{b}^2}{8\tilde{a}^2}, \quad Q = \sqrt[3]{\frac{\Delta_1 + \sqrt{\Delta_1^2 - 4\Delta_0^3}}{2}} \quad (48)$$

while the parameters Δ_0 and Δ_1 are:

$$\begin{aligned} \Delta_0 &= \tilde{c}^2 - 3\tilde{b}\tilde{d} + 12\tilde{a}\tilde{e}, \\ \Delta_1 &= 2\tilde{c}^3 - 9\tilde{b}\tilde{c}\tilde{d} + 27\tilde{b}^2\tilde{e} + 27\tilde{a}\tilde{d}^2 - 72\tilde{a}\tilde{c}\tilde{e}. \end{aligned} \quad (49)$$

In summary, the solution to the tuning of the resonant shunt circuit can be written in terms of the original parameters δ , r and α by considering Equations (50) to (53). From the knowledge of the coupling factor α , h_0 and χ are computed:

$$h_0 = \frac{8}{\alpha \sqrt{2\sqrt{54\alpha^4 - 144\alpha^2 + 64} + 9\alpha^2 + 16}}, \quad (50)$$

$$\chi = \frac{1}{8} \sqrt{64 - 2\alpha^2\sqrt{54\alpha^4 - 144\alpha^2 + 64} + 55\alpha^4 - 144\alpha^2}. \quad (51)$$

The coefficients of the quartic polynomials (41) are then calculated:

$$\begin{aligned} \tilde{a} &= \frac{(h_0^2 - 1)^2}{h_0^6}, \\ \tilde{b} &= -2 \frac{(2\chi + \alpha^2)(h_0^2 - 1)}{h_0^4}, \\ \tilde{c} &= 5 \frac{\alpha^4}{h_0^2} + \left(\frac{4\chi}{h_0^2} - \frac{8}{h_0^2} \right) \alpha^2 + \frac{6}{h_0^2} - \frac{6}{h_0^4}, \\ \tilde{d} &= 2\chi^3 + \left(4\alpha^2 - 2 - \frac{2}{h_0^2} \right) \chi - 2 \frac{\alpha^2}{h_0^2} + 2\alpha^6 - 2\alpha^4, \\ \tilde{e} &= \frac{1}{h_0^2}. \end{aligned} \quad (52)$$

From these coefficients, variables Δ_0 , Δ_1 , p , Q and S in Equations (48) and (49) are determined. The optimal parameters can then be obtained:

$$\delta_{opt} = 2 \sqrt{\frac{\tilde{a}}{4S\tilde{a} - \tilde{b}}}, \quad r_{opt} = \sqrt{\frac{2 [1 + (\delta_{opt}^2 + 1)(\alpha^2 + \chi - 1)h_0^2]}{[1 + (\chi\delta_{opt}^2 - 1)h_0^2]\delta_{opt}^2}} \quad (53)$$

The resistance R and inductance L of the shunt circuit are calculated directly from r_{opt} and δ_{opt} using Equations (14):

$$L = \frac{1}{\delta_{opt}^2 (1 + \kappa) \epsilon_3^T} \left(\frac{s_{33} l_0}{s_0} \right)^2, \quad (54)$$

$$R = \frac{r_{opt}}{\epsilon_3^T} \sqrt{\frac{m_1}{1 + \kappa}} \sqrt{s_{33}} \left(\frac{l_0}{s_0} \right)^3. \quad (55)$$

4.2 Numerical results

The transfer function of the primary oscillator (18) is computed for the optimal values proposed by the three tuning rules investigated in this paper:

$$\delta_{opt,H} = \delta_{opt,Y} = 1, \quad \delta_{opt,exact} = 2 \sqrt{\frac{\tilde{a}}{4S\tilde{a} - \tilde{b}}} \quad (56)$$

$$r_{opt,H} = \sqrt{2}\alpha, \quad r_{opt,Y} = \sqrt{\frac{r_P^2 + r_Q^2}{2}} = \frac{\sqrt{3}\alpha}{\sqrt{2 - \alpha^2}} \quad (57)$$

$$r_{opt,exact} = \sqrt{\frac{2 [1 + (\delta^2 + 1) (\alpha^2 + \chi - 1) h_0^2]}{[1 + (\chi \delta^2 - 1) h_0^2] \delta^2}} \quad (58)$$

These values are plotted in Figure 4 as a function of the dimensionless coupling parameter α within its allowable domain.

Figures 5-8, which depict the transfer functions for four different values of α , fully validate the analytic developments carried out in the previous section. Indeed, the transfer function for the exact rule possesses two resonance peaks with identical amplitude. The corresponding amplitude is also consistently lower than the maximum peak amplitude given by the other tuning rules.

For a very low value of the coupling parameter, $\alpha=0.01$ in Figure 5, there is almost no visible difference between Yamada and exact rules. The damping value proposed by Hagood's formula is associated with a noticeable performance decrease. For $\alpha = 0.1$ and $\alpha = 0.3$ in Figures 6-7, respectively, both Hagood and Yamada rules lead to lower performance compared to the exact rule. Finally, for $\alpha = 0.7$ in Figure 8, a complete detuning is observed for Yamada's rule. For a more quantitative comparison, Figure 9 displays the percentage of peak amplitude reduction provided by the exact rule as a function of α . It confirms the superiority of this tuning methodology over the existing methods. For realistic values of α , an improvement of a couple of percents can be expected.

5 Simplification of the exact formulas

Because expressions (50)-(53) are quite involved, the curves $\delta_{opt} = \delta_{opt}(\alpha)$ and $r_{opt} = r_{opt}(\alpha)$ in Figure 4 are fitted using fifth and third-order polynomials:

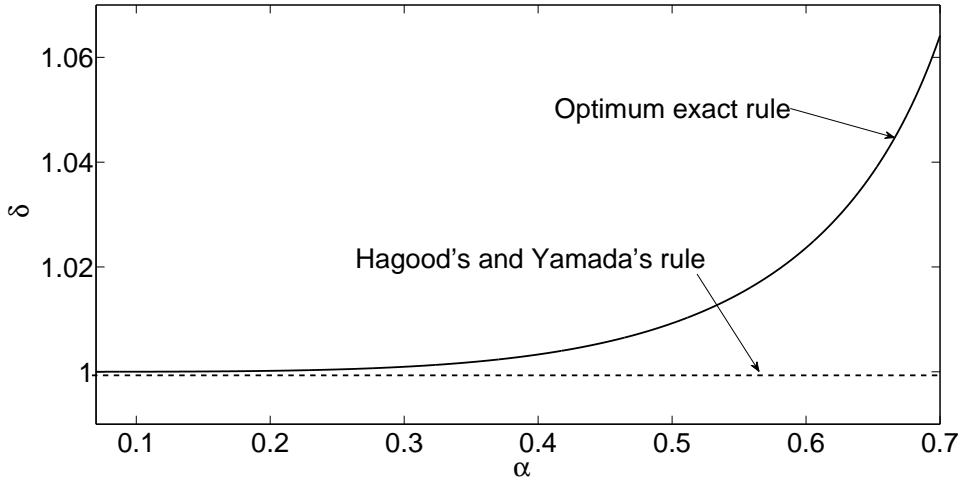
$$\hat{\delta}_{opt} = 1 + (a_5 \alpha^5 + a_4 \alpha^4 + a_3 \alpha^3 + a_2 \alpha^2 + a_1 \alpha + a_0), \quad (59)$$

$$\hat{r}_{opt} = n_3 \alpha^3 + n_2 \alpha^2 + n_1 \alpha + n_0. \quad (60)$$

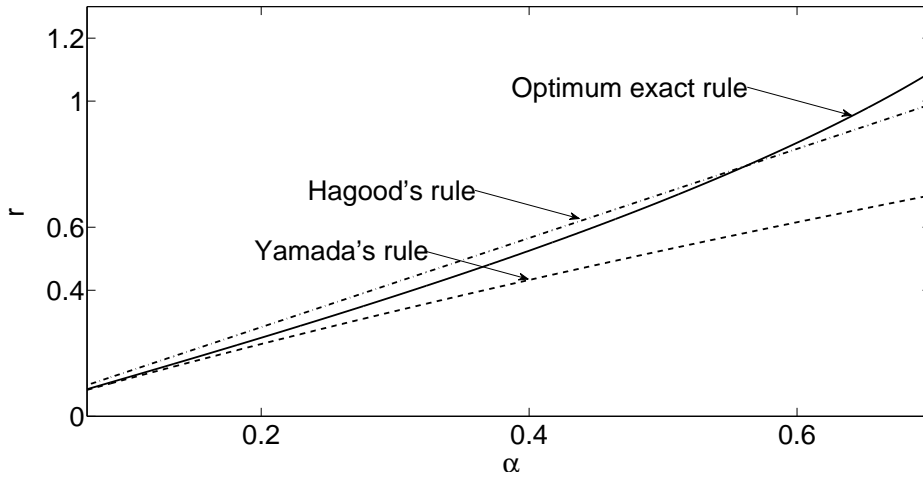
The coefficients a_i ($i=0, 1, 2, \dots, 5$) and n_j ($j=0, 1, 2, 3$) are listed in Tables 3 and 4, respectively.

Table 5 compares the exact and fitted values of the design parameters δ and r together with the corresponding maximum amplitude of the receptance function h_0 . The maximum

1
2
3
4
5
6
7
8
9
10
11
12
13
14
15
16
17
18
19
20
21
22
23
24
25
26
27
28
29
30
31
32
33
34
35
36
37
38
39
40
41
42
43
44
45
46
47
48
49
50
51
52
53
54
55
56
57
58
59
60

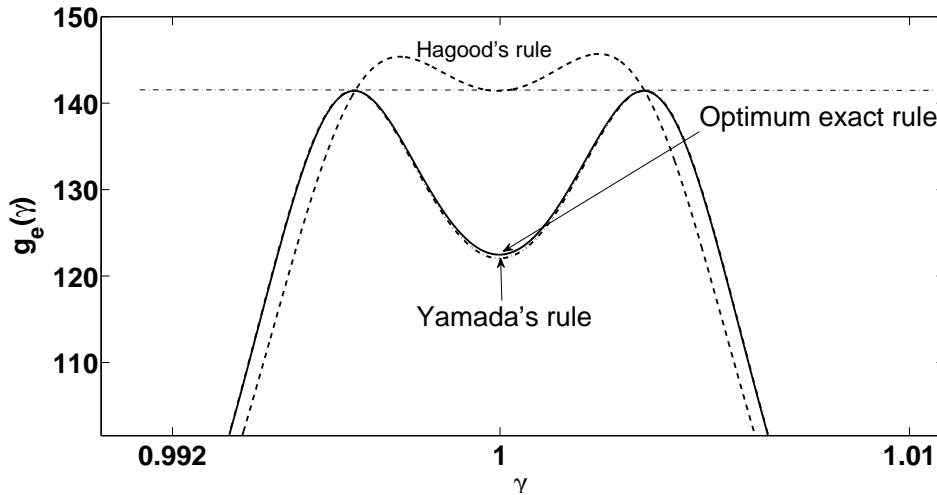


(a)

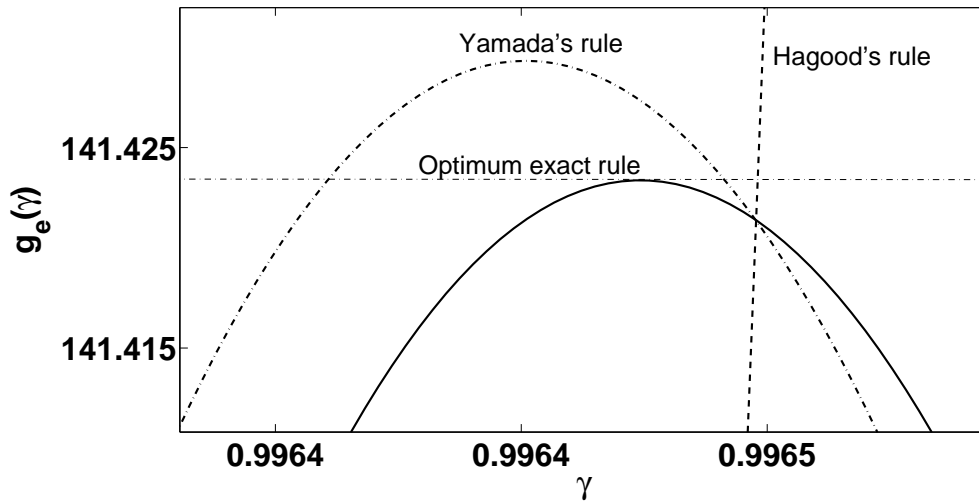


(b)

Figure 4: Variation of (a) the tuning frequency ratio δ , and (b) the dimensionless damping of the shunt r predicted by the different tuning rules against the electromechanical coupling parameter α .



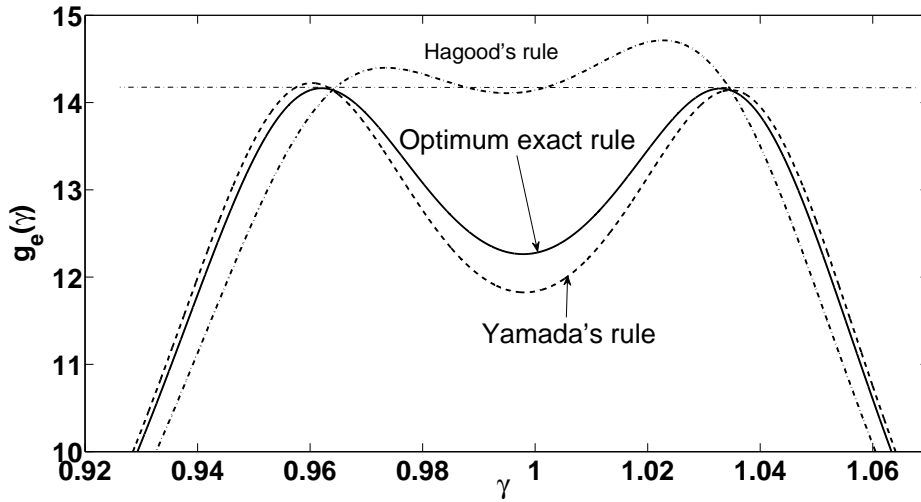
(a)



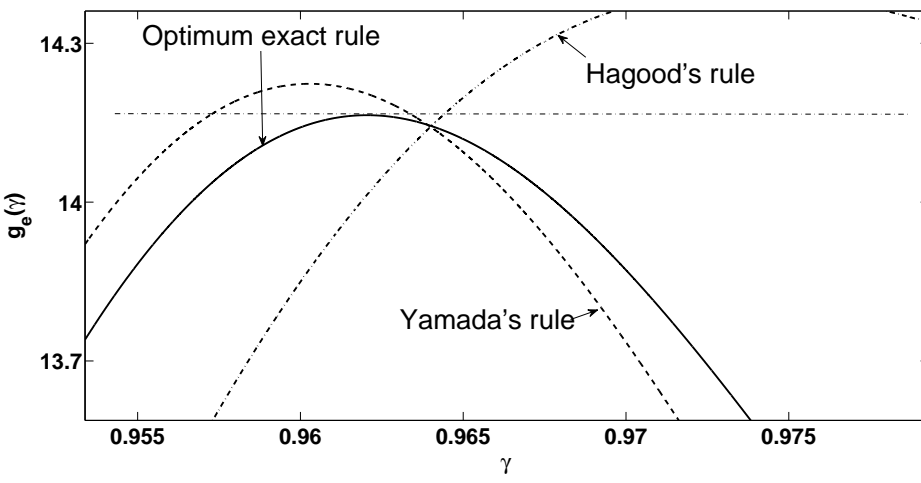
(b)

Figure 5: (a) Performance of the three tuning rules for $\alpha = 0.01$, (b) close-up of the resonant peak.

1
2
3
4
5
6
7
8
9
10
11
12
13
14
15
16
17
18
19
20
21
22
23
24
25
26
27
28
29
30
31
32
33
34
35
36
37
38
39
40
41
42
43
44
45
46
47
48
49
50
51
52
53
54
55
56
57
58
59
60



(a)



(b)

Figure 6: (a) Performance of the three tuning rules for $\alpha = 0.1$, (b) close-up of the resonant peak.

1
2
3
4
5
6
7
8
9
10
11
12
13
14
15
16
17
18
19
20
21
22
23
24
25
26
27
28
29
30
31
32
33
34
35
36
37
38
39
40
41
42
43
44
45
46
47
48
49
50
51
52
53
54
55
56
57
58
59
60

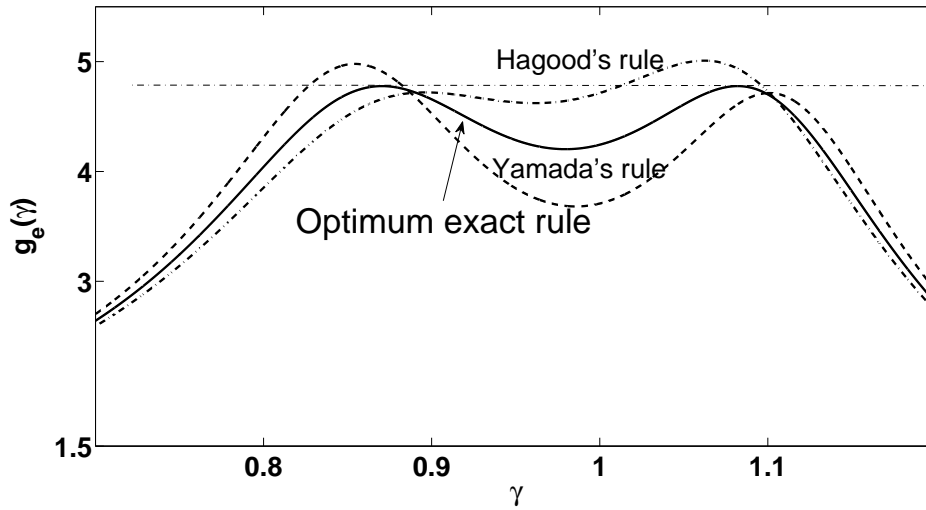


Figure 7: Performance of the three tuning rules for $\alpha = 0.3$.

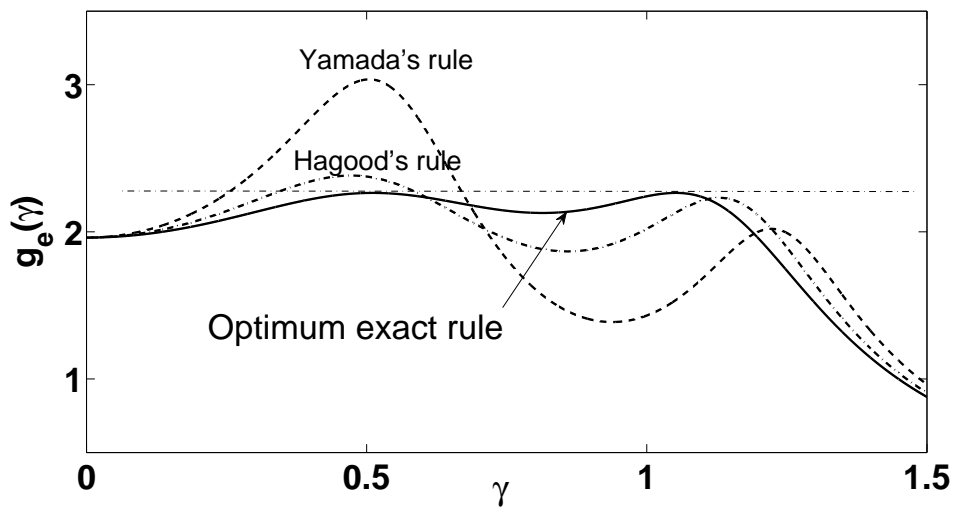


Figure 8: Performance of the three tuning rules for $\alpha = 0.7$.

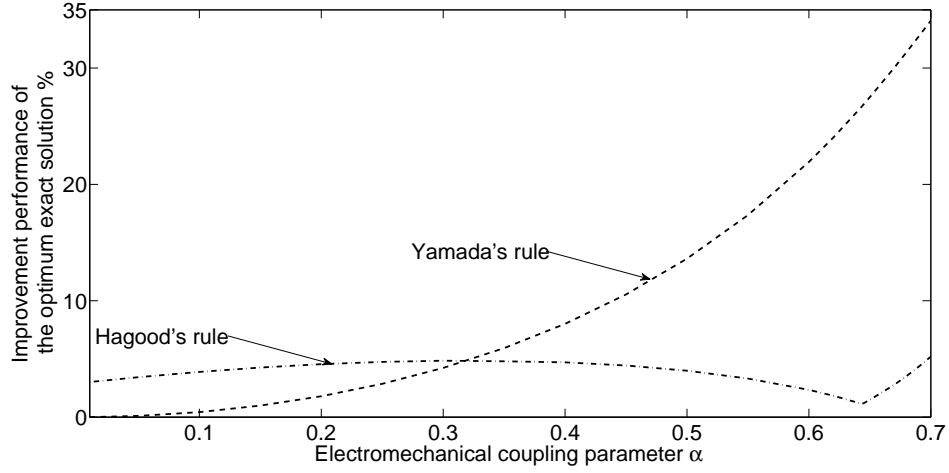


Figure 9: Percentage of peak amplitude reduction provided by the exact closed-form solution against the dimensionless coupling parameter α .

relative error on δ and r is 0.04% and 0.2%, respectively. Figure 10 depicts the comparison between the exact and fitted transfer functions for different dimensionless coupling parameters α . Overall, these results demonstrate the very high accuracy of the proposed simplifications (59)-(60).

Table 3: The coefficients a_i in Equation (59)

$\hat{\delta}$	a_5	a_4	a_3	a_2	a_1	a_0
$\alpha \leq 0.2$	0.09225	0.0808	0.00294	0	0	0
$\alpha > 0.2$	4.26314	-6.4942	3.9275	-1.0805	0.1335	-0.005771

Table 4: The coefficients n_i in Equation (60)

\hat{r}	n_3	n_2	n_1	n_0
$\alpha \leq 0.2$	0.5256	-0.00092	1.2247	0
$\alpha > 0.2$	1.17861	-0.5223	1.35353	-0.00901

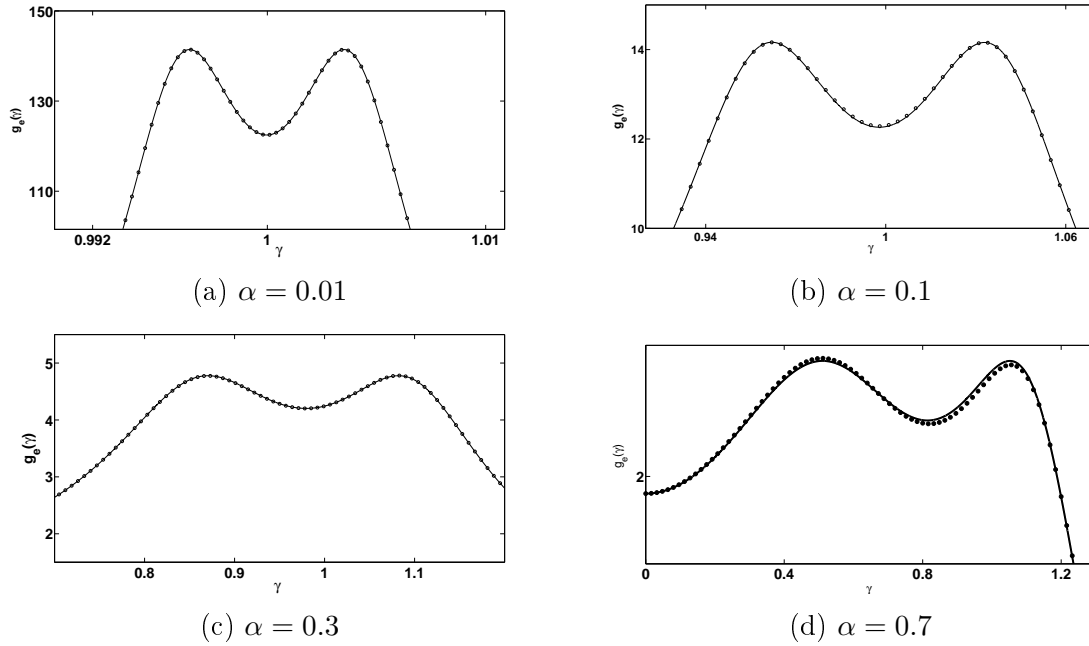


Figure 10: Receptance transfer function for the exact (solid line) and fitted (circles) values of δ_{opt} and r_{opt} for different dimensionless coupling parameters α .

Table 5: Exact and fitted values of δ_{opt} , r_{opt} and h_0 .

α	δ	$\hat{\delta}$	r	\hat{r}	h_0	\hat{h}_0
0.001	1.0000000	1.0000000	0.0012	0.0012	1414.2	1414.2
0.005	1.0000000	1.0000000	0.0061	0.0061	282.8433	282.8434
0.01	1.0000000	1.0000000	0.0122	0.0122	141.4233	141.4234
0.02	1.0000000	1.0000000	0.0245	0.0245	70.7146	70.7148
0.05	1.0000001	1.0000001	0.0613	0.0613	28.2942	28.2945
0.1	1.0000107	1.0000119	0.1230	0.1230	14.1621	14.1624
0.2	1.0001767	1.0001824	0.2492	0.2491	7.1118	7.1123
0.3	1.0009511	1.0008329	0.3819	0.3819	4.7772	4.7753
0.4	1.0033006	1.0035120	0.5254	0.5243	3.6242	3.6283
0.5	1.0092485	1.0091271	0.6848	0.6845	2.9482	2.9481
0.6	1.0236558	1.0235424	0.8680	0.8697	2.5200	2.5174
0.65	1.0380200	1.0384762	0.9728	0.9738	2.3705	2.3697

6 Conclusion

In this paper, an exact closed-form solution to the H_∞ optimization of piezoelectric material shunted with inductive-resistive passive electrical circuits is proposed. This solution imposes exactly two equal peaks in the receptance function that are associated with the smallest possible vibration amplitude of the host structure. The performance of this

1
2
3
4
5
6
7 method is therefore superior to all existing tuning rules for resonant circuit shunting,
8 even if the improvement may be marginal for small electromechanical coupling parame-
9 ters. Simplified, though very accurate, formulas for the optimum tuning ratio and the
10 dimensionless damping are also provided.
11

12 13 14 **7 Acknowledgments** 15 16

17
18 All authors, P. Soltani, G. Tondreau, A. Deraemaeker and G. Kerschen, would like to ac-
19 knowledge the financial support of the Belgian National Science Foundation FRS-FNRS
20 (PDR T.0028.13). The author G. Kerschen would like to acknowledge the financial sup-
21 port of the European Union (ERC Starting Grant NoVib 307265).
22
23

24 25 **References** 26 27

- 28
29 [1] J. Sun, M. R. Jolly, and M. Norris, “Passive, adaptive and active tuned vibration
30 absorbers-a survey,” *Journal of mechanical design*, vol. 117, no. B, pp. 234–242,
31 1995.
32
- 33 [2] J. P. Den Hartog, *Mechanical vibrations*. McGraw-Hill, 1934.
34
- 35 [3] J. Brock, “A note on the damped vibration absorber,” *Journal of Applied Mechanics*,
36 vol. 13, p. A284, 1946.
37
- 38 [4] O. Nishihara and T. Asami, “Closed-form solutions to the exact optimizations of dy-
39 namic vibration absorbers (minimizations of the maximum amplitude magnification
40 factors),” *Journal of Vibration and Acoustics*, vol. 124, no. 4, pp. 576–582, 2002.
41
- 42 [5] T. Asami, O. Nishihara, and A. Baz, “Analytical solutions to H_∞ and H_2 optimiza-
43 tion of dynamic vibration absorbers attached to damped linear systems,” *Journal of*
44 *Vibration and Acoustics*, vol. 124, no. 4, pp. 284–295, 2002.
45
46
- 47 [6] S. Mohameini, “A survey of recent innovations in vibration damping and control using
48 shunted piezoelectric transducers,” *IEEE Transactions on Control Systems Technol-*
49 *ogy*, vol. 11, no. 4, pp. 482–494, 2003.
50
51
- 52 [7] N. W. Hagood and A. von Flotow, “Damping of structural vibrations with piezo-
53 electric materials and passive electrical networks,” *Journal of Sound and Vibration*,
54 vol. 146, no. 2, pp. 243–268, 1991.
55
- 56 [8] A. Preumont, *Mechatronics: Dynamics of Electromechanical and Piezoelectric Sys-*
57 *tems*. Springer, 2006.
58
59
- 60 [9] G. S. Agnes and D. J. Inman, “Nonlinear piezoelectric vibration absorbers,” *Smart*
Materials and Structures, vol. 5, no. 5, p. 704, 1996.

- 1
2
3
4
5
6
7 [10] B. Zhou, F. Thouverez, and D. Lenoir, “Essentially nonlinear piezoelectric shunt
8 circuits applied to mistuned bladed disks,” *Journal of Sound and Vibration*, vol. 333,
9 no. 9, pp. 2520–2542, 2014.
- 10
11 [11] P. Soltani, G. Tondreau, A. Deraemaeker, and G. Kerschen, “Linear and nonlinear
12 piezoelectric shunting strategies for vibration mitigation,” in *International Confer-*
13 *ence on Structural Nonlinear Dynamics and Diagnosis, Agadir, Morocco*, 2014.
- 14
15 [12] H. Yu and K. Wang, “Piezoelectric networks for vibration suppression of mistuned
16 bladed disks,” *Journal of Vibration and Acoustics*, vol. 129, no. 5, pp. 559–566, 2007.
- 17
18 [13] B. Mokrani, R. Bastait, R. Vigié, and A. Preumont, “Vibration damping of tur-
19 bomachinery components with piezoelectric transducers: Theory and experiment,”
20 in *International Conference on Noise and Vibration Engineering, Leuven, Belgium*,
21 2012.
- 22
23 [14] E. M. Qureshi, X. Shen, and J. Chen, “Vibration control laws via shunted piezoelectric
24 transducers: A review,” *International Journal of Aeronautical and Space Sciences*,
25 vol. 15, no. 1, pp. 1–19, 2014.
- 26
27 [15] J. Hogsberg and S. Krenk, “Balanced calibration of resonant shunt circuits for piezo-
28 electric vibration control,” *Journal of Intelligent Material, Systems and Structures*,
29 vol. 23, no. 17, pp. 1937–1948, 2012.
- 30
31 [16] K. Yamada, H. Matsuhisa, H. Utsuno, and K. Sawada, “Optimum tuning of series and
32 parallel LR circuits for passive vibration suppression using piezoelectric elements,”
33 *Journal of Sound and Vibration*, vol. 329, no. 24, pp. 5036–5057, 2010.
- 34
35 [17] H. Frahm, “Device for damping vibrations of bodies,” tech. rep., US No. Patent
36 989958, 1909.
- 37
38 [18] J. Ormondroyd and J. Den Hartog, “The theory of the dynamic vibration absorber,”
39 *Transaction of the ASME*, vol. 50, pp. 9–22, 1928.
- 40
41 [19] T. Meeker, “Publication and proposed revision of ANSI/IEEE standard 176-1987,
42 ANSI/IEEE standard on piezoelectricity,” *IEEE Transactions on Ultrasonics Ferro-*
43 *electrics and Frequency Control*, vol. 43, no. 5, pp. 717–772, 1996.
- 44
45
46
47
48
49
50
51
52
53
54
55
56
57
58
59
60